

© Images courtesy of Daniel Einstein

# Multiscale Modeling of the Primary Visual Cortex

## *Modeling of Neuronal Network Dynamics*

BY AADITYA V. RANGAN,  
LOUIS TAO,  
GREGOR KOVACIC,  
AND DAVID CAI

The extraordinary power of the brain is apparent from the vast complexity of its behaviors and the ease with which it performs them. These behaviors are accomplished by a complex system of excitatory and inhibitory neurons of different types, operating with large intrinsic fluctuations, through extensive feedback, and often with competition between many scales in space and time. The behavior of such large-scale neuronal systems is simply not understood; however, today, a combination of modern experiments, large-scale scientific computation, and mathematical modeling and analysis begins to offer us a glimpse of the inner workings of some parts of this fascinatingly complex system.

One of the best-studied parts of the brain is the primary visual cortex (V1). Along the visual pathway, it is in V1 where neuronal responses are first simultaneously selective to elementary features of the visual scene, including the orientation of lines and edges, their location, and sharpness. In other words, it is in V1 where the first simple, but nontrivial, neuronal computations take place, eventually giving rise to the visual percept when their results are relayed to the higher visual areas and beyond.

A classical property of V1 is orientation tuning, the selective response of a single neuron to some orientations of a simple visual pattern (e.g., an edge, bar, or grating), but not to other orientations, which was first revealed in microelectrode measurements of spiking activity [1], [2]. Neuronal orientation preference in V1 is organized into millimeter-scale orientation hypercolumns [3] of like orientation preference laid out in regular patterns, with spokes that emanate from pinwheel centers. In contrast, spatial phase preference appears not to have a well-organized distribution across V1 [4].

Recent advances in optical imaging with voltage-sensitive dyes have revealed new dynamic information encoded as spatiotemporal patterns of cortical activity on scales beyond those that can be observed by traditional experimental methods. Two striking recent examples are the observed patterns of spontaneous cortical activity [5], [6] and the cortical dynamics corresponding to the Hikosaka line-motion illusion [7], [8]. Such spatiotemporal activity presents intriguing possibilities of functional significance for sensory information processing [9].

Our modeling of neuronal response properties in V1 has revealed a possible distinctive dynamical state or operating state of V1, from which it responds to changes in visual stimulation. In this article, we unify the results obtained from our large-scale, physiologically realistic, yet minimal computational V1 network models [10]–[12] and identify a single cortical operating state, namely, an intermittent desuppressed state (IDS) with fluctuation-controlled criticality. This state dynamically controls various aspects of important model V1 responses. In particular, within this single operating state, our network dynamics has successfully reproduced combined results of real-time optical imaging on spatiotemporal cortical activity patterns [5]–[7] and of single unit recordings revealing detailed firing-rate information from individual neurons relevant to orientation tuning [13]–[18]. We have also proposed possible network and synaptic mechanisms underlying these cortical phenomena.

### Methods

Our model neuronal networks are composed of single-compartment, conductance-based, integrate-and-fire, point neurons, of which approximately 75% are excitatory and 25% are inhibitory [10]–[12]. The neurons within V1 are driven by external stimuli through the lateral geniculate nucleus (LGN), which is responsible for the organization of both orientation preference and spatial phase preference within V1. The orientation preference is laid out in pinwheel patterns, and the preferred spatial phase varies randomly from neuron to neuron. Spikes incoming to V1 from the LGN and background noise are modeled as independent Poisson spike trains to each cell.

Every model V1 neuron has local isotropic and nonspecific connections sparsely projecting to other nearby V1 neurons. The excitatory and inhibitory connections are mediated by  $\alpha$ -amino-3-hydroxyl-5-methyl-4-isoxazole-propionate (AMPA) and  $\gamma$ -aminobutyric acid (GABA<sub>A</sub>) type receptors, respectively, with respective conductance decay time scales of approximately 3 and 8 ms [19]. Local monosynaptic inhibition and excitation have length scales shorter than that of a single orientation hypercolumn, approximately 500  $\mu\text{m}$ . Long-range (approximately 1,500  $\mu\text{m}$ ) connections terminate at both fast AMPA and slow *N*-methyl-*D*-aspartic acid (NMDA) (approximately 80–200 ms) receptors of both excitatory and inhibitory

Digital Object Identifier 10.1109/MEMB.2009.932803

## Spatiotemporal activity presents intriguing possibilities of functional significance for sensory information processing.

neurons. These connections are excitatory and orientation-specific; i.e., connecting only neurons with similar orientation preference [20].

Our model includes simple and complex cells, distinguished by the amount of LGN drive they receive, with the simple cells receiving more drive. Our model reproduces the classical behavior of their spatial summation properties: simple cell responses are linear, and complex cell responses are nonlinear [12].

Our model neurons (with simulations containing up to approximately  $10^6$  neurons) are uniformly distributed over a cortical area (spanning up to  $25 \text{ mm}^2$ ). Simple and complex cells are randomly distributed in space. At the cortical scales examined in our model, retinotopic effects can be neglected. Our networks are effective or lumped models of V1, since we do not include the detailed laminar structure of V1 in our modeling.

### Fluctuation-Controlled Criticality

Our extensive simulations have revealed an operating state of our model cortex, namely, a state near a fluctuation-controlled criticality [12]. We first illustrate it for a highly idealized, statistically uniformly, sparsely connected network model. In this model, one half of the neurons, i.e., simple cells, receive feedforward drive in the form of uniform Poisson spike trains with identical rates and spike strengths, while the other half, i.e., complex cells, receives a strong intracortical excitation. The inhibitory cells provide strong intracortical inhibition to other cells in the network.

Figure 1 describes this network's bifurcation structure present in the average firing rate of an excitatory complex cell as a function of the average driving strength to the simple cells

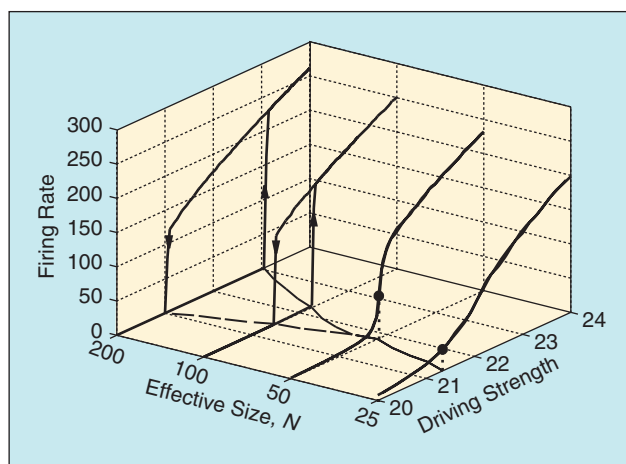


**Fig. 1.** Bifurcation diagram near the fluctuation-controlled criticality in an idealized network. (Reproduced with permission from [12], [www.pnas.org](http://www.pnas.org); Copyright 2007, National Academy of Sciences, USA.)

(i.e., the product of the Poisson rate and spike strength of the feedforward drive trains) and of the effective network size  $N$  (i.e., the average number of presynaptic neurons coupled to a given neuron, which can be controlled by connectivity sparsity). As we vary  $N$ , and thus the variance of synaptic conductances, the gain curve exhibits a transition to bistability and hysteresis. At the critical point where bistability first occurs, the gain in the response curve is the most rapid. In addition to network sparseness, this criticality can also be controlled by the NMDA/AMPA ratio in excitatory conductances. We operate our model V1 networks just below this critical point to obtain steep gain on the one hand and sufficiently high intrinsic fluctuations on the other, so that the network avoids the unphysiological, bistability-induced instability.

### Orientation Tuning Via a Local Model

To investigate neuronal orientation tuning in V1, we model a  $1\text{-mm}^2$  local patch, incorporating only short-range cortico-cortical connections and covering four orientation hypercolumns that contain approximately  $10^4$  model neurons [12]. We constrain it to function in an operating state just below the fluctuation-controlled criticality. This state is characterized by high total conductance with strong corticocortical inhibition as well as large synaptic conductance and membrane potential fluctuations achieved through sparsity in network connectivity. The average neuronal membrane potentials in the network remain well below the spiking threshold; thus, the spiking is caused by strong, sparsity-induced synaptic fluctuations in the network. The model network gives rise to a continuum of simple and complex cells, as characterized by the modulation ratio  $F_1/F_0$  of the cell's cycle-averaged firing rate, which is the ratio between its first Fourier component and its mean at a preferred stimulus orientation. For the population of our V1 neurons, this ratio has a bimodal distribution, whereas the corresponding  $F_1/F_0$  of the intracellular voltages has a unimodal distribution in agreement with the experimental results of [13] and [14].

A quantitative measure of orientation selectivity for drifting grating stimuli is given by circular variance (CV) [12]. The CV lies between 0 and 1, and it is near 0 for well-tuned and near 1 for poorly tuned neurons. Figure 2(a) shows the CV distributions of the simple and complex excitatory cells in our model. Both types of cells are well tuned, their distributions are broad, and the simple cells appear to be moderately better tuned than the complex cells. Figure 2(b) demonstrates the approximate contrast invariance of orientation selectivity of our model neurons. Figure 2(c) shows that orientation selectivity for the firing rates is almost independent of the neuron's location within the orientation column. The neuronal conductances in our model are tuned more broadly in cells near the pinwheel centers than in isoorientation domains. All these

**Our model neurons (with simulations  
containing up to approximately  $10^6$  neurons)  
are distributed over a cortical area  
spanning up to  $25 \text{ mm}^2$ .**

results are in good agreement with experimental observations in [15]–[18]. As pointed out in [12], sparsity-induced near criticality plays a crucial role in producing physiologically realistic orientation tuning dynamics within our V1 model.

### Spatiotemporal Activity: Spontaneous Patterns and Line-Motion Illusion

#### Spontaneous Patterns of Cortical Activity

Experiments on anesthetized cats, described in [5] and [6], show that spontaneous cortical activity of single V1 neurons forms intriguing coherent patterns, persisting more than 80 ms on the spatial scales of several millimeters, appearing in regions of similar orientation preference over many orientation hypercolumns. To investigate the network mechanisms underlying these patterns, we incorporated both isotropic and lateral long-range corticocortical connections (the latter being orientation specific and containing both fast AMPA and slow NMDA components) in our large-scale (approximately  $10^6$  neurons) network model of V1 and examined their dynamical consequences [10].

To quantify our numerical observations, we follow [5] and [6] and consider the preferred cortical state of a neuron, defined as the average of the voltage snapshots taken over the network at the firing times of this neuron while the network is driven by a strong stimulus at this neuron's preferred orientation. In addition, for the same neuron, we consider the spike-triggered spontaneous activity pattern, which is the analogous voltage snapshot average taken in the network without an external stimulus.

Our study reveals the mechanism underlying the spontaneous cortical activity patterns, which is characterized by an IDS state. This IDS operating state is an intermittent cycle: during periods of strong cortical inhibition and after its decay, neurons in an isoorientation domain become correlated in subthreshold activity, so a spontaneous firing of a single excitatory neuron will recruit many other neurons to fire within a few milliseconds. This recruitment rapidly spreads to neurons in other isoorientation domains of like preference via the long-range connections, by significantly elevating the highly correlated NMDA conductances and voltages in these domains within approximately 1 mm. As a result, the induced spatial patterns of the voltage closely resemble the orientation preference map and the preferred cortical state. The excitatory recruitment events trigger strong inhibition mediated by local connections, which suppresses any further recruitment. The pattern then slowly drifts or decays on the NMDA conductance decay scale, which is approximately 80 ms, and the inhibition decays with it, hence giving rise to a possible initiation of another cycle of this kind. These cycles persist intermittently through the evolution of the model V1 dynamics. The NMDA component present in the long-range corticocortical connections is crucial for ensuring the correct spatiotemporal scales of the activity patterns.

In Figure 3(a), we display the neuronal orientation preference as conferred on the V1 neurons by their afferent LGN input to which we compare two instantaneous patterns of spontaneous cortical activity within our IDS operating state [Figure 3(b) and (c)]. In Figure 3(b), the regions of high

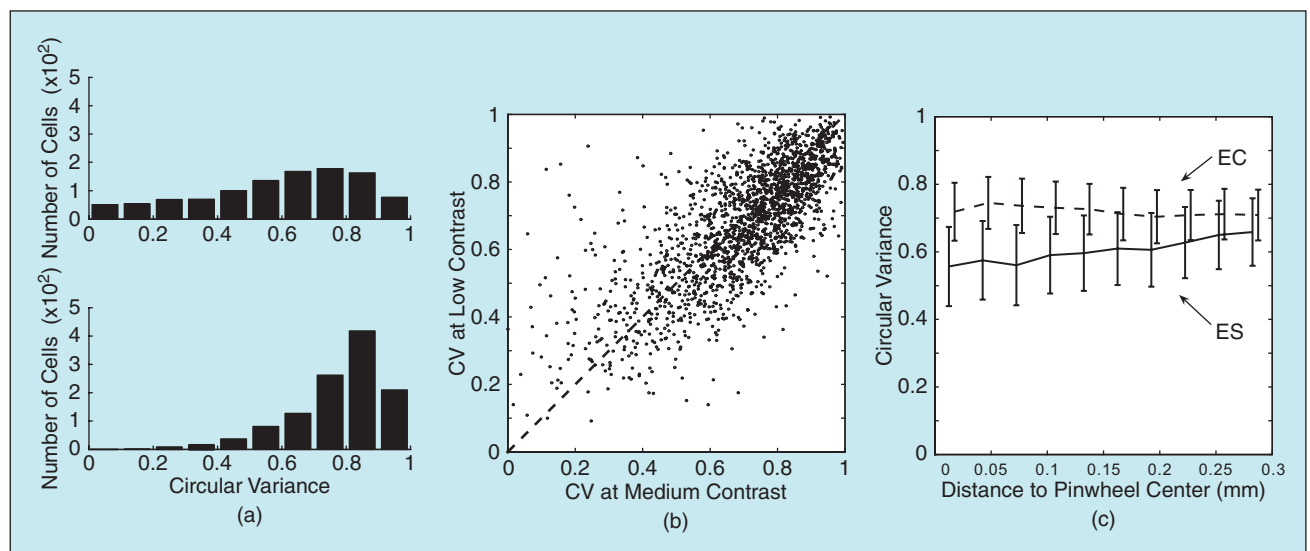


**Fig. 2.** (a) CV histograms for excitatory simple (top) and complex (bottom) cells. (b) CV at medium versus low contrasts. (c) Dependence of CV on the distance from a pinwheel center: EC and ES are excitatory complex and simple cells, respectively. (Reproduced with permission from [12], www.pnas.org; Copyright 2007, National Academy of Sciences, USA.)

activity cover isoorientation domains belonging to predominantly one preferred angle, while those in Figure 3(c) belong to two angles and are thus largely separate, with an occasional

small penetration into each-other's territory. Spatially separated isoorientation regions tend to become activated simultaneously and persist for approximately 80 ms before switching to neighboring orientations, in agreement with experimental observations [5], [6].

In the IDS operating state, our model cortex reproduces the experimental observation [5], [6] that the measures of the preferred cortical state and the spike-triggered spontaneous activity pattern strongly resemble one another, as seen in Figure 4(a) and (b). Both of them have a strong correlation with the neuronal orientation preference map from Figure 3(a).

To measure the predominant time scale of the patterns, we compute the similarity index (SI),  $\rho$ , defined as the instantaneous spatial correlation between a neuron's preferred cortical state and the

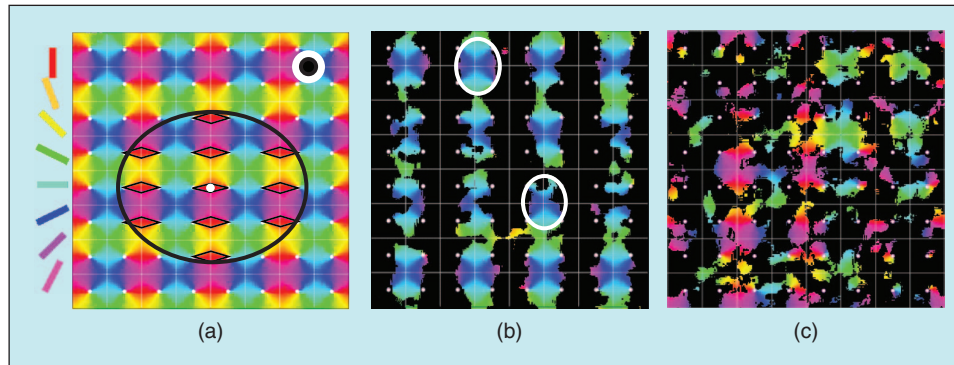


**Fig. 3.** (a) Orientation hypercolumns, with preferred neuronal orientation denoted by the color. Small white dots: pinwheel centers. Black/white annulus inner/outer radius: length scale of local inhibitory or excitatory couplings. Large ellipse: extent of long-range connections. Rhombuses: orientation domains coupled by the long-range connections to the neurons in the orientation domain in the middle of the ellipse. (b) and (c) Two instantaneous spontaneous activity patterns. The two ovals in (b) represent regions in which membrane potentials can be highly correlated in time. (Reproduced with permission from [10], www.pnas.org; Copyright 2007, National Academy of Sciences, USA.)

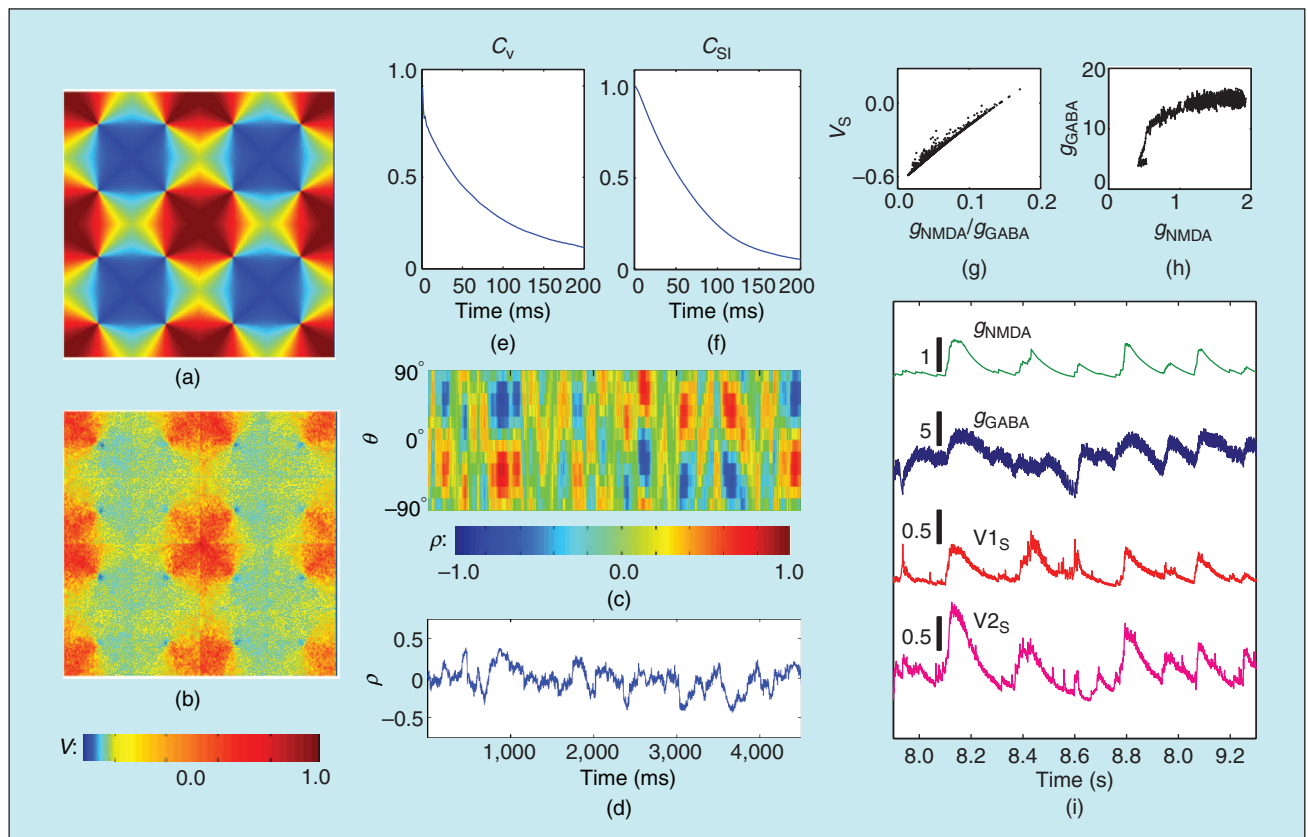


**Fig. 4.** (a) Preferred cortical state of the neuron in the middle of the plot. (b) Spike-triggered activity pattern of the same neuron. (c) Evolution of the SI over time and orientation preference. (d) Evolution of the SI over time for orientation preference  $-60^\circ$ . (e) and (f) Autocorrelations of the membrane potential and SI. (g) and (h) Correlations of the effective reversal potential, NMDA, and inhibitory (GABA) conductances. (i) Typical time traces of NMDA and GABA conductances (top two traces) and membrane potentials of two neurons that are approximately 1.0 mm apart (bottom two traces). The approximate 80-ms correlation times are clearly discernible from (c), (e), (f), and (i). (Reproduced with permission from [12] and [13], www.pnas.org; Copyright 2007, National Academy of Sciences, USA.)



## Sparsity-induced near criticality plays a crucial role in producing physiologically realistic orientation tuning dynamics within our V1 model.

membrane potential of the neurons in the network. Its time evolution is shown in Figure 4(c), and its time trace at  $\theta = -60^\circ$  in Figure 4(d). Both indicate that the typical pattern duration to be approximately 80 ms, which is also visible from the temporal autocorrelation functions shown in Figure 4(e) and (f). The network operates in a state of high total conductance with strong inhibition. The membrane potential,  $V$ , the effective reversal potential,  $V_S$ , and the NMDA conductances are all highly correlated, as can be seen from Figure 4(g)–(i). The voltages generally stay well below the firing threshold. A near synchronization of neuronal membrane potentials within approximately 1 mm [see Figure 4(i)] occurs even when the neurons are not spiking and is caused by the common synaptic inputs from long-range connections. These dynamical properties of the membrane potential evolution in our network are consistent with the experimental observations [5], [6].

Importantly, the IDS state not only captures the spontaneous dynamics but also generates physiologically observed spatiotemporal responses under external stimuli. We comment that other operating states (such as the state of marginal mode [21]) have not produced spontaneous cortical activity patterns with correct spatial and temporal scales as observed experimentally. In particular, spontaneous cortical activity arising in a marginal state often produces an overly excitatory dynamics, leading to runaway instability, if an external stimulation is applied.

### Line-Motion Illusion

The Hikosaka line-motion illusion stimulus consists of a small stationary square flashed on a display for approximately 50 ms, followed by an adjacent stationary bar [8], creating the illusion that the bar continuously grows out of the square. Optical imaging experiments using voltage-sensitive dye reveal that this stimulus creates an activity pattern in V1 that closely resembles the pattern created by a small moving square [7]. This close resemblance is likely linked to the preattentive perception of illusory motion.

We simulated the V1 activity patterns associated with this illusion using our model

cortex operating in the IDS state [11]. We calibrated the strength of our model LGN by comparing the V1 activity of our model cortex and the experimental signal obtained for a flashed square, as displayed in Figure 5(a)–(c). In Figure 5(d)–(k), we next present the cortical activity patterns evoked by the moving square and the Hikosaka stimulus. The spatiotemporal profiles of the effective reversal potential are in good qualitative agreement with the experimental signal. In the IDS state, the NMDA conductance is strongly correlated with the membrane potential in our model, as seen in Figure 5(f), (g), (j), and (k). The moving square produces a rightward growing area of activity that fills out its path [Figure 5(e), (f), and (g)]. The Hikosaka stimulus (square followed by a bar) produces a rightward growing area of activity, which starts growing near the area of activity evoked by the square [Figure 5(i)–(k)]. The dynamics of the two activity patterns, both in the model and the real V1, are remarkably similar, and this similarity may be associated with the illusory motion perception.

Our computations reveal the network mechanism underlying the spatiotemporal activity associated with the line-motion illusion. The LGN input modulation due to the square causes recruitment in the immediate cortical area corresponding to the square. The neuronal spiking due to this recruitment causes the increase of the NMDA conductance in neurons that can be

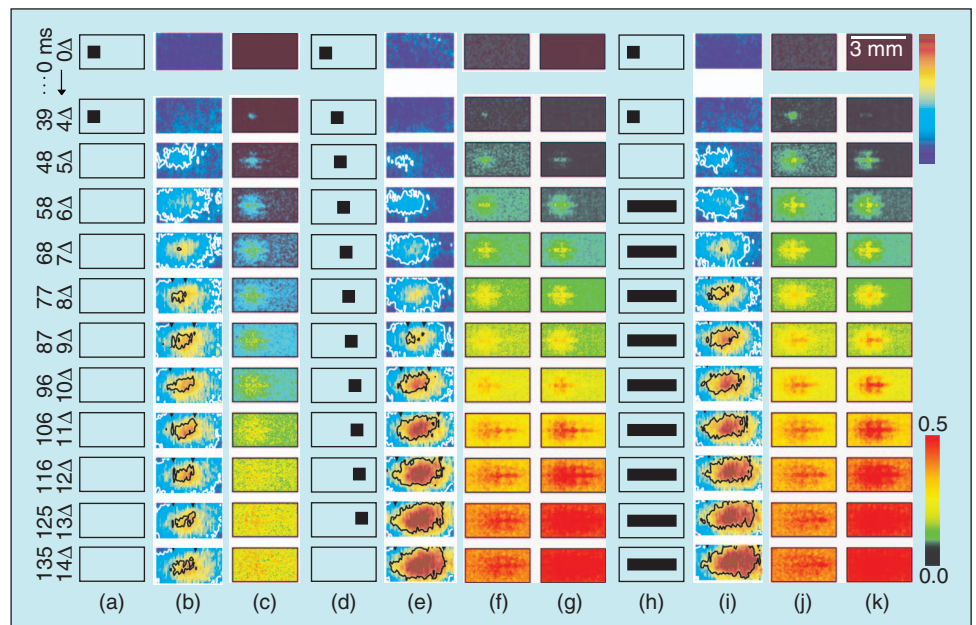


**Fig. 5.** Cortical activity corresponding to the (a) flashed and (d) moving square, and (h) Hikosaka stimuli. (b), (e), and (i) Signal measured in the experiments. (Reproduced with permission from [7]; Copyright 2004, Macmillan Publishers Ltd.) (c), (f), and (j) Effective reversal potentials in our model. (g) and (k) NMDA conductances in our model. (Reproduced with permission from [11], [www.pnas.org](http://www.pnas.org); Copyright 2007, National Academy of Sciences, USA.)

reached from the recruited area by the long-range connections in the IDS state. This increase persists for approximately 80 ms after the initial LGN input modulation has subsided. Because of the correlation between the membrane potentials and NMDA conductances in the IDS state, the membrane potentials of these neurons are also elevated but stay below the firing threshold, because long-range connections are not strong enough to cause spiking by themselves. When the LGN input modulation due to the bar arrives, spiking initiates in this already primed cortical area near the trace of the square, because of the already elevated activity. This firing sends additional activity, via the long-range NMDA connections, into the unprimed region affected by the bar, which causes a wave of activity growing along the V1 area corresponding to the bar away from the V1 area corresponding to the square.

The crucial ingredients of the underlying network mechanism are the spatiotemporal input profile sculpted by the model LGN, the facilitative effect of the long-range NMDA corticocortical conductances that is induced by the (square) cue, and the strong correlation between the neuronal NMDA conductances and membrane potentials that exist in the IDS operating state.

## Discussion

By modeling V1 dynamics as revealed by intracellular and extracellular measurements of orientation tuning dynamics [13]–[18] and optical imaging of large-scale spatiotemporal cortical patterns using voltage-sensitive dyes [5]–[7], our study suggests a possible operating state of V1 characterized by high total conductance with strong inhibition, large synaptic fluctuations, and the important role played by the NMDA conductance in long-range, orientation-specific interactions [10]–[12]. All of these ingredients appear essential for the stable operation of the model cortex and its ability to quantitatively and qualitatively reproduce a host of dynamical phenomena exhibited by the real cortex. The network mechanisms as revealed in the IDS state with fluctuation-controlled criticality in our model V1 dynamics, in turn, may offer suggestions for the physiological underpinnings of the neuronal dynamics in real V1.



**Aaditya V. Rangan** received his Ph.D. degree in mathematics from the University of California, Berkeley, in 2003. He is an assistant professor of mathematics at New York University. His research interests include mathematical neuroscience and large-scale scientific computing.



**Louis Tao** received his Ph.D. degree in physics from the University of Chicago in 1995. He is a principal investigator at the Center of Bioinformatics at Peking University. His research interests are in mathematical neuroscience and computational biology.



**Gregor Kovacic** received his Ph.D. degree in applied mathematics from Caltech in 1989. He is an associate professor of mathematical sciences at Rensselaer Polytechnic Institute. His research interests include nonlinear optics and mathematical neuroscience.



**David Cai** received his Ph.D. degree in physics from Northwestern University in 1994. He is a professor of mathematics at New York University. His research interests include nonlinear, stochastic processes in physical and biological sciences and mathematical neuroscience.

**Address for Correspondence:** David Cai, Courant Institute of Mathematical Sciences, New York University, 251 Mercer St., New York, NY 10012, USA. E-mail: cai@cims.nyu.edu.

## References

- [1] D. Hubel and T. Wiesel, "Receptive fields, binocular interaction and functional architecture of the cat's visual cortex," *J. Physiol.*, vol. 160, no. 1, pp. 106–154, 1962.
- [2] D. Hubel and T. Wiesel, "Receptive fields and functional architecture of the monkey striate cortex," *J. Physiol.*, vol. 195, no. 1, pp. 215–243, 1968.
- [3] T. Bonhoeffer and A. Grinvald, "Iso-orientation domains in cat visual cortex are arranged in pinwheel like patterns," *Nature*, vol. 353, no. 6343, pp. 429–431, 1991.
- [4] G. DeAngelis, R. Ghose, I. Ohzawa, and R. Freeman, "Functional micro-organization of primary visual cortex: Receptive field analysis of nearby neurons," *J. Neurosci.*, vol. 19, no. 10, pp. 4046–4064, 1999.
- [5] M. Tsodyks, T. Kenet, A. Grinvald, and A. Arieli, "Linking spontaneous activity of single cortical neurons and the underlying functional architecture," *Science*, vol. 286, no. 5446, pp. 1943–1946, 1999.
- [6] T. Kenet, D. Bibitchkov, M. Tsodyks, A. Grinvald, and A. Arieli, "Spontaneously emerging cortical representations of visual attributes," *Nature*, vol. 425, no. 6961, pp. 954–956, 2003.
- [7] D. Jancke, F. Chavance, S. Naaman, and A. Grinvald, "Imaging cortical correlates of illusion in early visual cortex," *Nature*, vol. 428, no. 6981, pp. 423–426, 2004.
- [8] O. Hikosaka, S. Miyauchi, and S. Shimojo, "Focal visual attention produces illusory temporal order and motion sensation," *Vis. Res.*, vol. 33, no. 9, pp. 1219–1240, 1993.
- [9] A. Grinvald, A. Arieli, M. Tsodyks, and T. Kenet, "Neuronal assemblies: Single cortical neurons are obedient members of a huge orchestra," *Biopolymers*, vol. 68, no. 3, pp. 422–436, 2003.
- [10] D. Cai, A. V. Rangan, and D. W. McLaughlin, "Architectural and synaptic mechanisms underlying coherent spontaneous activity in V1," *Proc. Natl. Acad. Sci. USA*, vol. 102, no. 16, pp. 5868–5873, 2005.
- [11] A. V. Rangan, D. Cai, and D. W. McLaughlin, "Modeling the spatiotemporal cortical activity associated with the line-motion illusion in primary visual cortex," *Proc. Natl. Acad. Sci. USA*, vol. 102, no. 52, pp. 18793–18800, 2005.
- [12] L. Tao, D. Cai, D. W. McLaughlin, M. J. Shelley, and R. Shapley, "Orientation selectivity in visual cortex by fluctuation-controlled criticality," *Proc. Natl. Acad. Sci. USA*, vol. 103, no. 34, pp. 12911–12916, 2006.
- [13] D. Ringach, R. Shapley, and M. Hawken, "Orientation selectivity in macaque V1: Diversity and laminar dependence," *J. Neurosci.*, vol. 22, no. 13, pp. 5639–5651, 2002.
- [14] N. Priebe, F. Mechler, M. Carandini, and D. Ferster, "The contribution of spike threshold to the dichotomy of cortical simple and complex cells," *Nat. Neurosci.*, vol. 7, no. 10, pp. 1113–1122, 2004.
- [15] P. Maldonado, I. Godecke, C. Gray, and T. Bonhoeffer, "Orientation selectivity in pinwheel centers in cat striate cortex," *Science*, vol. 276, no. 5318, pp. 1551–1555, 1997.
- [16] J. Shummers, J. Marino, and M. Sur, "Synaptic integration by V1 neurons depends on location within the orientation map," *Neuron*, vol. 36, no. 5, pp. 969–978, 2002.
- [17] J. Marino, J. Shummers, D. C. Lyon, L. Schwabe, O. Beck, P. Wiesing, K. Obermayer, and M. Sur, "Invariant computations in local cortical networks with balanced excitation and inhibition," *Nat. Neurosci.*, vol. 8, no. 2, pp. 194–201, 2005.
- [18] J. Anderson, I. Lampl, D. Gillespie, and D. Ferster, "The contribution of noise to contrast invariance of orientation tuning in cat visual cortex," *Science*, vol. 290, no. 5498, pp. 1968–1972, 2000.
- [19] C. Koch, *Biophysics of Computation*. Oxford: Oxford Univ. Press, 1999.
- [20] A. Angelucci, J. Levitt, E. Walton, J.-M. Hupe, J. Bullier, and J. Lund, "Circuits for local and global integration in primary visual cortex," *J. Neurosci.*, vol. 22, no. 19, pp. 8633–8646, 2002.
- [21] J. A. Goldberg, U. Rokni, and H. Sompolinsky, "Patterns of ongoing activity and the functional architecture of the primary visual cortex," *Neuron*, vol. 13, no. 3, pp. 489–500, 2004.